Supporting Information for

The molecular architecture of photoreceptor phosphodiesterase 6 (PDE6) with activated G protein elucidates the mechanism of visual excitation

Michael J. Irwin, Richa Gupta, Xiong-Zhuo Gao, Karyn B. Cahill, Feixia Chu, Rick H. Cote

This PDF file includes:

Table S1. PDE6 holoenzyme crosslinked peptides and identification scores.

pep1	aa1	pep2	aa2	score	fragment 1	fragment 2
Pβ	471	Pβ	475	31.1	E(+EDC)R	LGK(+EDC)EPADC(Carbamidomethyl)EEDELGK
Pβ	675	Pβ	813	10.6	K(+EDC)R	ALADE(+EDC)YEAK
Pβ	675	Pβ	815	20.0	K(+EDC)R	ALADEYE(+EDC)AK
Pβ	823	Pβ	832	18.4	ALEE(+EDC)DQK	KETTAK(+EDC)K
Pβ	824	Pβ	832	11.2	ALEED(+EDC)QK	KETTAK(+EDC)K
Pβ	825	Pβ	827	24.1	ALEEDQ(+User Defined Link)K	K(+User Defined Link)ETTAK
Pβ	826	Pβ	828	22.2	ALEEDQK(+User Defined Link)K	E(+User Defined Link)
Pβ	826	Pβ	829	23.4	ALEEDQK(+User Defined Link)K	ET(+User Defined Link)TAK
Pβ	826	Pβ	831	22.8	ALLEDQJ(+User Defined Link)K	ETTA(+User Defined Link)K
Pβ	826	Pα/Pβ	445/444	23.7	ALEEDQK(+User Defined Link)K	LENR(+User Defined Link)K
Pβ	826	Pα/Pβ	442/441	20.1	ALEEDQK(+User Defined Link)K	L(+User Defined Link)ENRK
Pβ	826	Pβ	828	30.4	ALEEDQK(+EDC)K	E(+EDC)TTAKK
Pβ	826	Pα/Pβ	444/443	17.7	ALEEDQK(+User Defined Link)K	LENR(+User Defined Link)K
Pβ	826	Pβ	832	14.5	ALEEDQK(+User Defined Link)K	ETTAK(+User Defined Link)K
Pγ	1	Pβ	78	23.9	(+DSS)-MNLEPPKAEIR	VVFK(+DSS)ILR
Pγ	C2	Pβ	84	15.4	VMC(+User Defined Link)GPVTPRKGPPK	C(+User Defined Link)SLFMYR
Pγ	4	Pβ	146	19.8	MNLE(+EDC)PPK	DIGVVGHVAQTK(+EDC)
Pγ	7	Pβ	184	19.8	MNLE(+EDC)PPK	DIGVVGHVAQTK(+EDC)
Pγ	C18	Pα	383	7.5	VMC(+User Defined Link)GPVTPRKGPPK	ELDESGWMFK(+User Defined Link)
Pγ	C18	Pβ	92	9.9	VMC(+User Defined Link)GPVTPRKGPPK	C(+User Defined Link)SLFMYR
Pγ	C18	Pα	233	7.6	VMC(+User Defined Link)GPVTPRKGPPK	VFHLSYLHNC(+User Defined Link)ETRR
Pγ	31	Pβ	200	8.3	KFK(+User Defined Link)QR	KLDPC(+User Defined Link)FTSEDEDVFLK
Pγ	41	Pα	469	17.8	QFKSK(+User Defined Link)PPK	C(Carbamidomethyl)DNEEIQTIL(+User Defined Link)K
Pγ	44	Pα/Pβ	613/611	15.8	GTNNLYQMK(+DSS)SQNPLAK	QFK(Xlink:DSS1)SKPPK(+DSS)K
Pγ	44	Pβ	475	24.5	QFKSK(+User Defined Link)PPK	C(Carbamidomethyl)DNEEIQTIL(+User Defined Link)K
Pγ	52	Pα/Pβ	328/326	16.4	QFK(Xlink:DSS1)SKPPK(+DSS)K	GTNNLYQMK(+DSS)SQNPLAK
Pγ	K62	Pβ	450	20.6	QFKSKPPK(+DSS)K	ERLGK(+DSS)EPADC(Carbamidomethyl)EEDELGK
Pγ	K62	Pβ	446	18.7	GVQGFGD(+EDC)	DYILHGKEDIK(+EDC)
Pγ	K62	Pα/Pβ	394	32.4	DDIPGMEGLGK(+EDC)	DIAQD(+EDC)MVLYHVRC(Carbamidomethyl)
Pγ	K62	Pα/Pβ	393	33.4	DDIPGMEGLGK(+EDC)	D(+EDC)IAQDMVLYHVRC(Carbamidomethyl)
Pγ	K65	Pα	767	18.0	DDIPGMKGLGK(+EDC)	KEE(+EDC)IVGVATFYNR
Pγ	C68	Pβ	839	22.8	DDIPGMKGLGK(+EDC)	KE(+EDC)EIVGVATFYNR

Refer to Table 1 for precursor charge and m/z for each cross-linked peptide.

Table S2. Gt_{α}-GDP-AlF_4^- and Pγ crosslinked peptides and identification scores

pep1	aa1	pep2	aa2	score	frag 1	frag 2
Gtα	16	Gtα	20	24.8	ELE(+EDC)KK	LK(+EDC)EDAEKDAR
Gtα	16	Gtα	25	22.3	ELE(+EDC)KK	LKEDAEK(+EDC)DAR
Gtα	17	Gtα	20	25.8	ELEK(+DSS)K	LK(+DSS)EDAEK
Gtα	17	Gtα	21	21.1	ELEK(+EDC)KLK	E(+EDC)DAEK
Gtα	17	Gtα	22	21.1	ELEK(+EDC)KLK	ED(+EDC)AEK
Gtα	17	Gtα	31	38.0	ELEK(+DSS)K	TVK(+DSS)LLLLGAGESGK
Gtα	18	Gtα	26	22.1	K(+EDC)LKEDAEK	D(+EDC)AR
Gtα	18	Gtα	31	39.2	K(+DSS)LK	TVK(+DSS)LLLLGAGESGK
Gtα	18	Gtα	267	26.1	K(+DSS)LK	K(+DSS)DVFSEK
Gtα	20	Gtα	31	40.4	LK(+DSS)EDAEKDAR	LK(+DSS)LLLLGAGESGK
Gtα	20	Gtα	205	18.7	LK(+DSS)EDAEK	K(+DSS)K
Gtα	21	Gtα	275	20.5	E(+User Defined Link)DAEKDAR	IK(+User Defined Link)K
Gtα	24	Gtα	31	39.2	LKEDAE(+EDC)K	TVK(+EDC)LLLLGAGESGK
Gtα	25	Gtα	31	42.8	LKEDAEK(+DSS)DAR	TVK(+DSS)LLLLGAGESGK
Gtα	25	Gtα	189	15.2	LKEDAEK(+EDC)DAR	D(+EDC)LNFR
Gtα	26	Gtα	31	38.8	D(+EDC)AR	TVK(+EDC)LLLLGAGESGK
Gtα	26	Gtα	205	17.6	D(+EDC)AR	SERK(+EDC)K
Gtα	39	Gtα	47	35.1	LLLLGAGE(+EDC)SGK	STMK(+EDC)QMK
Gtα	169	Gtα	176	44.2	VK(+EDC)TTGIIETQFSFK	LVTPGYVPTEQD(+EDC)VLR
Gtα	267	Gtα	275	25.1	K(+DSS)DVFSEK	IK(+DSS)K
Gtα	267	Gtα	342	9.2	K(+EDC)DVFSEK	E(+EDC)NLK
Gtα	98	Pγ	39	10.4	D(+EDC)DARK	EFK(+EDC)
Gtα	129	Pγ	25	13.3	D(+EDC)SGIQAC(Carbamidomethyl)FDR)	K(+EDC)GPPKFK
Gtα	203	Pγ	39	15.2	DVGGQRSE(+EDC)R	QFK(+EDC)
Gtα	203	Pγ	45	16.3	K(+EDC)GVQGFG	SE(+EDC)RKK

Refer to Table 2 for precursor charge and m/z for each cross-linked peptide.

Table S3. Gt_{α}-GDP-AlF_4^- and PDE6 holoenzyme activation complex crosslinked peptides and identification scores.

pep1	aa1	pep2	aa2	score	frag 1	frag 2
Gtα	9	Pα/Pβ	442/440	10.0	Acetyl-MGAGASAEE(+EDC)K	M(Oxidation)NK(+EDC)LENR
Gtα	10	Pβ	826	16.7	Xlink:DSS2-MGAGASAEEK(+User Defined Link)HSR	ALEEDQK(+User Defined Link)K
Gtα	10	Pα	854	7.2	Acetyl-MGAGASAEEK(+DSS)HSRELEKK	QPGGGPASK(+DSS)SC(Carbamidomethyl)C(Carbamidomethyl)VQ
Gtα	17	Pα	551	11.7	ELEK(BS3)K	FM(oxidation)YSLSK(BS3)GYR
Gtα	17	Pβ	817	23.3	ELEK(+User Defined Link)	ALADEYEAK(+User Defined Link)
Gtα	17	Pα/Pβ	808/806	5.7	ELEK(+EDC)K	E(+EDC)WK
Gtα	20	Pα/Pβ	807/805	12.7	LK(+DSS)EDAEKDARTVK	K(+DSS)EWK
Gtα	20	Pα/Pβ	620/618	10.1	LK(+DSS)EDAEK	SQNPLAK(+DSS)LHGSSILER
Gtα	24	Pα/Pβ	330/328	17.1	DYILHGKEDIK(+User Defined Link)VIPSPPA	DAE(+User Defined Link)K
Gtα	25	Pα	309	12.7	EDAEK(+EDC)DAR	TPD(+EDC)GREINFYK
Gtα	128	Pα/Pβ	807/805	15.6	LWK(+DSS)DSGIQAC(Carbamidomethyl)FDR	K(+DSS)EWEK
Gtα	275	Pβ	307	9.5	IK(EDC)K	TPD(EDC)GREILFYK
Gtα	98	Pγ	41	6.1	QD(+EDC)DAR	SK(+EDC)PPK
Gtα	275	Pγ	29	27.2	IK(+DSS)K	KGPPK(+DSS)FK
Pα/Pβ	328/326	Pγ	25	9.8	ED(EDC)IK	K(EDC)GPPK
Pα	551	Pγ	29	10.7	FM(oxidation)YSLSK(BS3)GYR	ELEK(BS3)K

Refer to Table 3 for precursor charge and m/z for each cross-linked peptide.

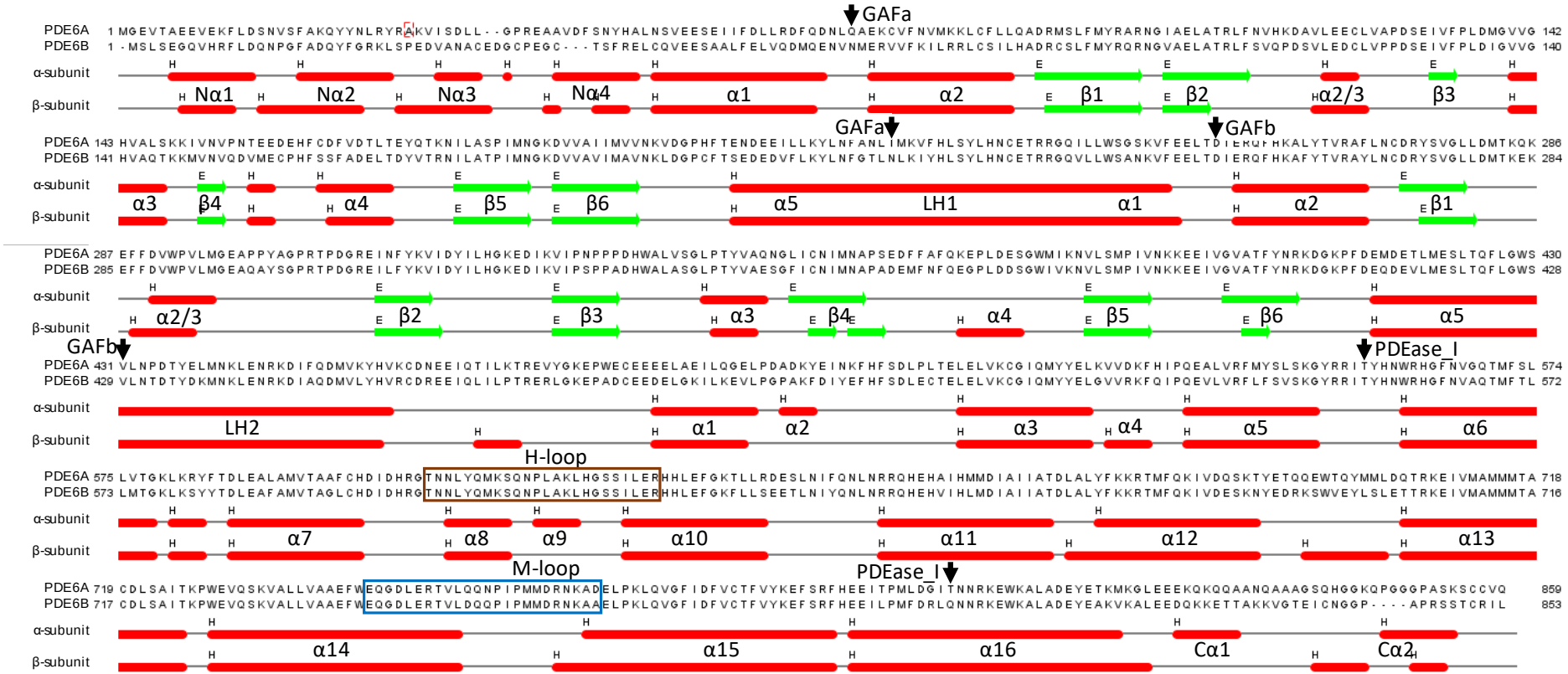

Fig. S1. Structural alignment of rod PDE6 catalytic subunits. Bovine rod photoreceptor α- and β-subunit sequences (PDE6A Uniprot accession number P11541; PDE6B Uniprot accession number P23439) were aligned and secondary structure elements (red, α-helix; green, β-strand) from our structural model shown below the sequence. The start and end of the tandem GAF domains (pfam accession number PF01590) and catalytic domains (PDEase_I accession number PF00233) are noted, along with the H- and M-loops (1). The numbering of the secondary structure elements for the GAF domains follows the convention in ref. (2), while the numbering scheme for the catalytic domain is derived from the structural alignment of the catalytic domains of multiple PDE families (4). Secondary structural elements in our cross-linked refined integrative structural model were validated with secondary structures obtained from the crystal structure of the cone PDE6C GAFa domain (5) and the cryo-EM structure of rod PDE6 (3).

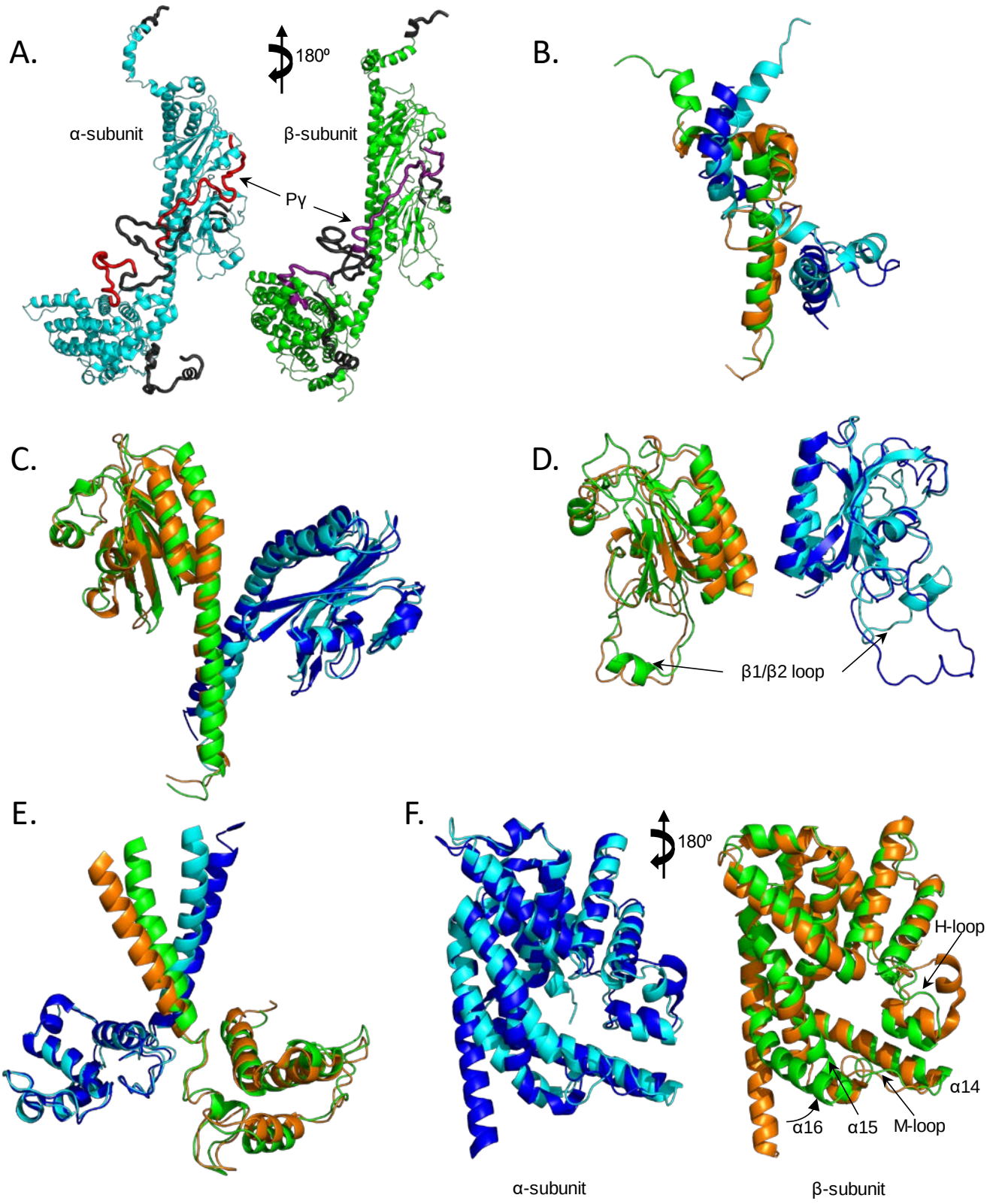

Fig. S2. New and refined structural elements of the catalytic and inhibitory subunits of PDE6 resolved by chemical crosslinking and integrative structural modeling. **A.** The α- (cyan) and β-subunit (green) with their associated Pγ subunit are shown highlighting in black the portions of each subunit that were not previously resolved in the 6MZB cryo-EM structure (3). **B.-F.** Differences between our structural model (cyan and green) and 6MZB (blue and orange) for the N-terminal region (B), GAFa domain (C), GAFb domain (D), the "linker" region connecting GAFb with the core catalytic domain (E) and the catalytic domain (shown as separate monomeric units for clarity, F).

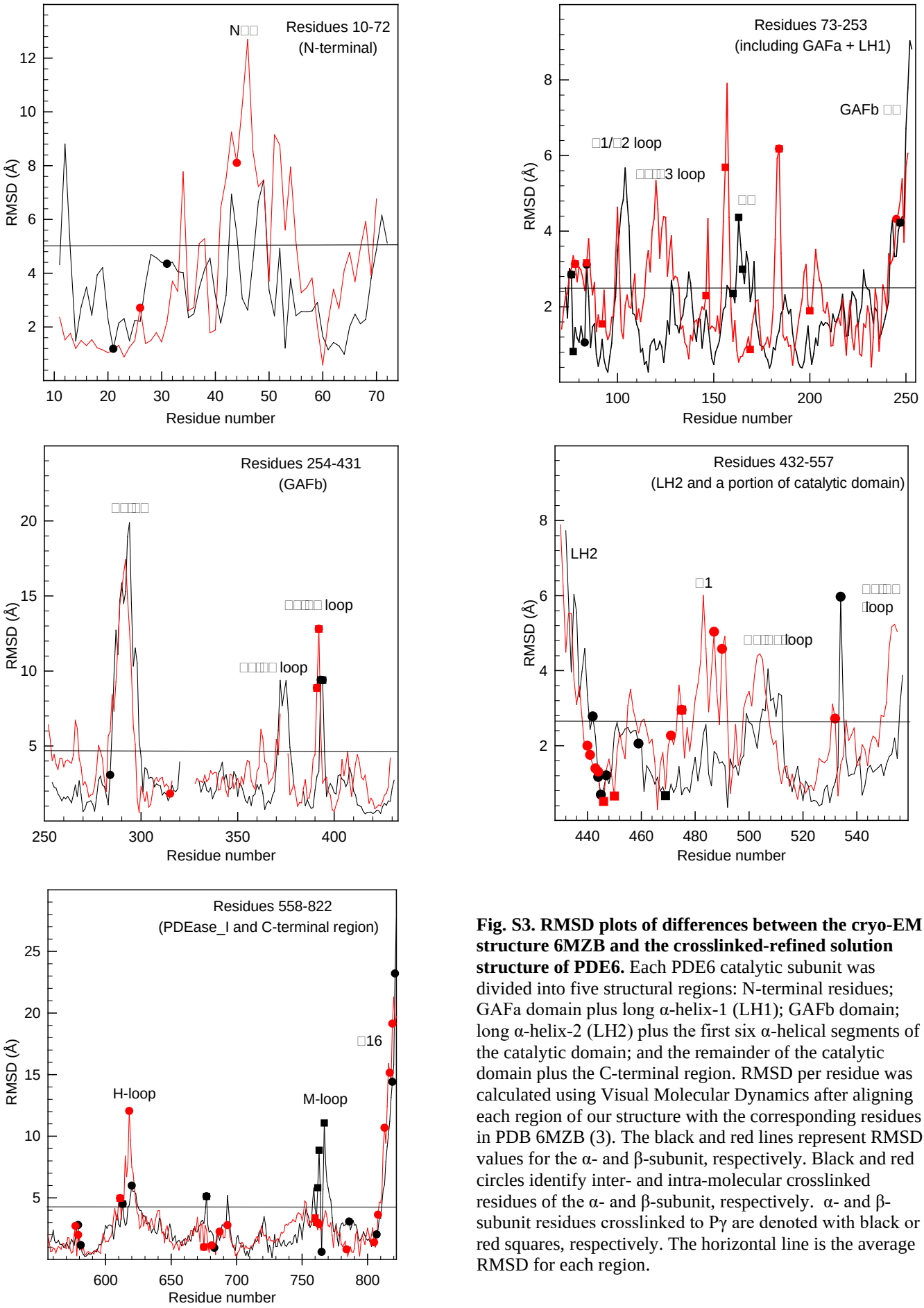

Fig. S3. RMSD plots of differences between the cryo-EM structure 6MZB and the crosslinked-refined solution structure of PDE6. Each PDE6 catalytic subunit was divided into five structural regions: N-terminal residues; GAFa domain plus long α-helix-1 (LH1); GAFb domain; long α-helix-2 (LH2) plus the first six α-helical segments of the catalytic domain; and the remainder of the catalytic domain plus the C-terminal region. RMSD per residue was calculated using Visual Molecular Dynamics after aligning each region of our structure with the corresponding residues in PDB 6MZB (3). The black and red lines represent RMSD values for the α- and β-subunit, respectively. Black and red circles identify inter- and intra-molecular crosslinked residues of the α- and β-subunit, respectively. α- and β-subunit residues crosslinked to Pγ are denoted with black or red squares, respectively. The horizontal line is the average RMSD for each region.

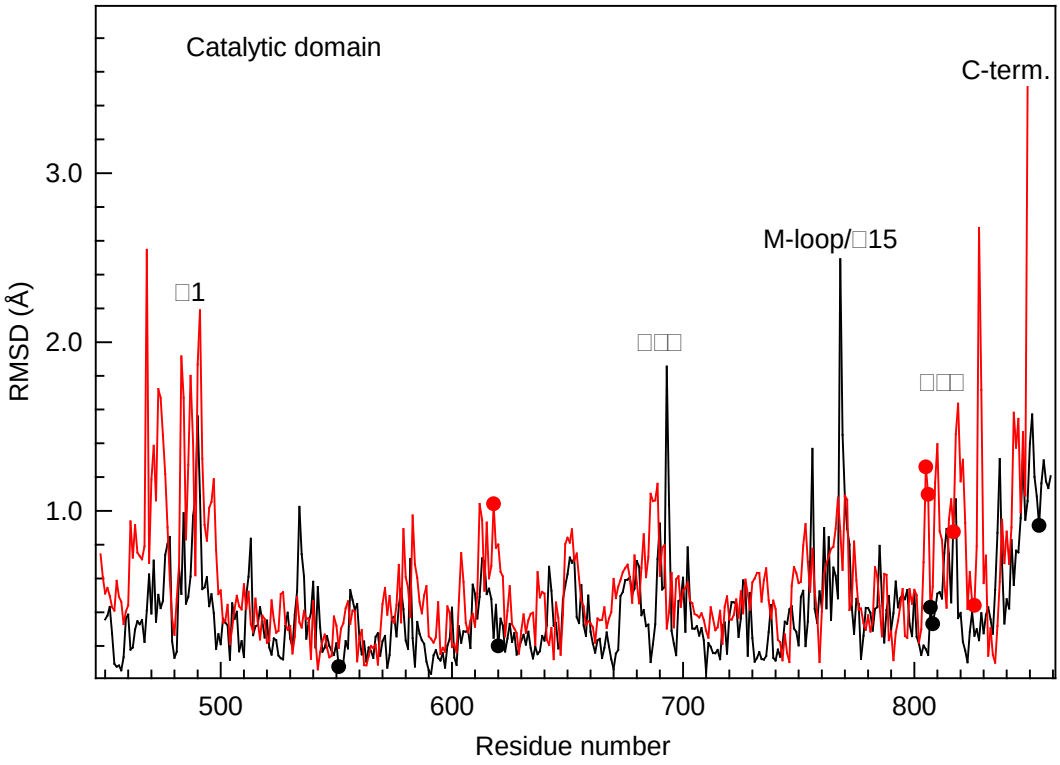

Fig. S4. RMSD plot comparing the catalytic domains of activated and nonactivated PDE6. RMSD per residue was calculated using Visual Molecular Dynamics after aligning the catalytic domains (including the C-terminal portion of the GAFb domains) of non-activated PDE6 holoenzyme with the corresponding residues in the transducin-activated PDE6 complex. The black and red lines represent RMSD values for the α-subunit (residues 455-859) and β-subunit (residues 448-852), respectively. Black and red circles identify inter-molecular crosslinked residues between the two Gt_{α} subunits and the α- and β-subunit, respectively. The overall RMSD was 0.5 Å for the α-subunit and 1.3 Å for the β-subunit.

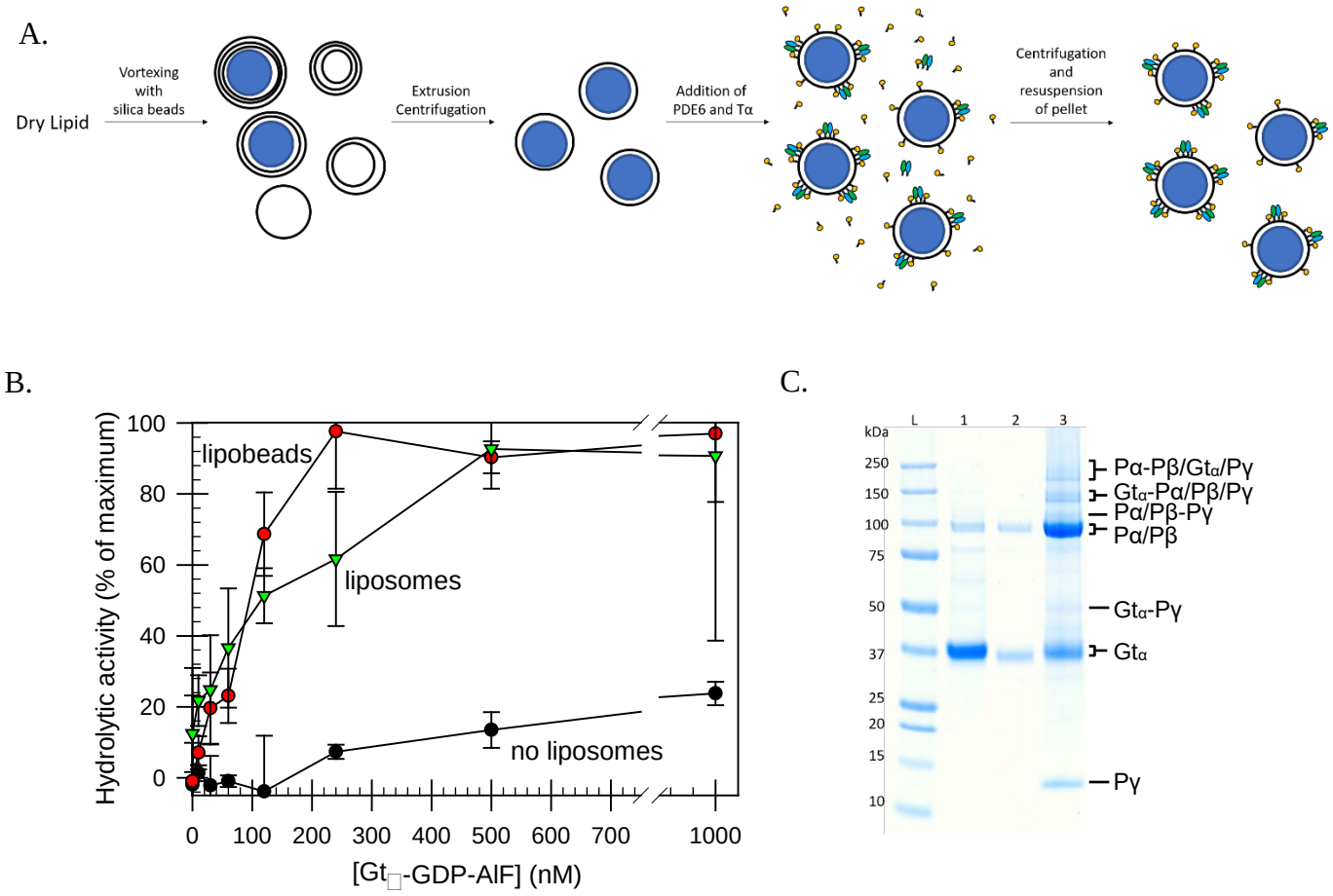

Fig S5. Preparation of DOTAP/DOPC-coated silica beads ("lipobeads") for studying transducin activation of PDE6 attached to liposomes. A. Schematic diagram of the process of generating DOPC/DOTAP-coated silica particles, membrane attachment of PDE6 holoenzyme and Gt_{α}-GDP-AlF_4^-, and removal of unbound proteins prior to initiating the cross-linking reaction. **B.** PDE6 holoenzyme (1 nM) was mixed with increasing concentrations of Gt_{α}-GDP- AlF_4^- in the absence of liposomes (black circles), in the presence of multi-lamellar vesicles prepared with DOPC/DOTAP (green triangles) or DOPC/DOTAP-coated lipobeads (red circles) **C.** SDS-PAGE illustrating removal of unbound proteins prior to crosslinking the lipobead-bound activated complex of Gt_{α}-GDP- AlF_4^- and PDE6. Lane 1 is the supernatant fraction following initial centrifugation of the lipobeads to remove unbound Gt_{α} (~37 kDa) and PDE6 catalytic subunits (~100 kDa). Lane 2 is the supernatant fraction after the crosslinking reaction was completed, while Lane 3 is the resuspended lipobead pellet containing the pulled-down crosslinked proteins that are excised from the gel for mass spectrometric analyses (*see Materials and Methods*).

References

1. Barren, B., Gakhar, L., Muradov, H., Boyd, K. K., Ramaswamy, S., and Artemyev, N. O. (2009) Structural basis of phosphodiesterase 6 inhibition by the C-terminal region of the γ-subunit. *EMBO J* **28**, 3613-3622
2. Heikaus, C. C., Pandit, J., and Klevit, R. E. (2009) Cyclic nucleotide binding GAF domains from phosphodiesterases: structural and mechanistic insights. *Structure* **17**, 1551-1557
3. Gulati, S., Palczewski, K., Engel, A., Stahlberg, H., and Kovacik, L. (2019) Cryo-EM structure of phosphodiesterase 6 reveals insights into the allosteric regulation of type I phosphodiesterases. *Sci Adv*. 10.1126/sciadv.aav4322
4. Ke, H., and Wang, H. (2007) Crystal structures of phosphodiesterases and implications on substrate specificity and inhibitor selectivity. *Curr. Top. Med. Chem* **7**, 391-403
5. Martinez, S. E., Heikaus, C. C., Klevit, R. E., and Beavo, J. A. (2008) The structure of the GAF A domain from phosphodiesterase 6C reveals determinants of cGMP binding, a conserved binding surface, and a large cGMP-dependent conformational change. *J. Biol. Chem* **283**, 25913-25919